Theoretical Analysis of Orientation Distribution Function Reconstruction of Textured Polycrystal by Parametric X-rays

I Lobach and A Benediktovitch

Physics Department, Belarusian State University, 4, Nezavisimosti Av., 220030, Minsk, Belarus

E-mail: `lobachihor@mail.ru`

Abstract. The possibility of quantitative texture analysis by means of parametric x-ray radiation (PXR) from relativistic electrons with Lorentz factor $\gamma > 50\text{MeV}$ in a polycrystal is considered theoretically. In the case of rather smooth orientation distribution function (ODF) and large detector ($\theta_D \gg 1/\gamma$) the universal relation between ODF and intensity distribution is presented. It is shown that if ODF is independent on one from Euler angles, then the texture is fully determined by angular intensity distribution. Application of the method to the simulated data shows the stability of the proposed algorithm.

1. Introduction

The orientation distribution function (ODF) of a polycrystalline material provides quantitative description of crystallograhic texture and enables to calculate the anisotropic physical properties of a polycrystalline material [1, 2]. There are several methods of quantitative texture analysis that provide the ODF. The most common is based on measurement of Bragg x-ray diffraction peak as a function of polycrystalline sample orientation, the so called pole figures. Provided with pole figures measured for several reciprocal lattice vectors there are several approaches to reconstruct the ODF [3–6]. The same methodology is used for processing the neutron diffraction data, the neutron technique being advantageous for large samples with coarse grains, e.g. geological samples [7]. Another widespread technique for quantitative texture analysis is electron backscattering diffraction (EBSD) [8]. This technique directly provides orientation of individual grains at the investigated cross section, unlike the x-ray and neutron diffraction techniques that provide the texture information in indirect way, but from large statistical ensemble of grains from the gauge volume.

Parametric x-ray radiation (PXR) is radiation in x-ray frequency range from relativistic electrons interacting with crystal target, the radiation parameters being directly related to crystallographical properties of the target [9]. Theoretical description [10, 11] and experiments [12–15] on PXR from a polycrystal show that there is a connection between texture of a polycrystal and PXR spectrum and intensity distribution. One of the obstacles in applications of PXR is its low total photon yield, however, the experiments [14, 15] revealed that the intensity of PXR from a polycrystalline Mo can be comparable with the intensity of its characteristic K_α-line. In the present contribution we investigate theoretically if it is feasible to perform quantitative texture analysis based on PXR data and to reconstruct the ODF.

2. Calculation of PXR from polycrystals

2.1. Basic relations for PXR in polycrystals

Orientation distribution function defines the volume part of crystallines having certain orientation:

$$\frac{dV}{V} = f(\varphi, \psi, \theta) \sin\theta d\varphi d\psi d\theta, \tag{1}$$

here φ, ψ, θ are the 3 Euler angles, see figure 1a; the blue coordinate system corresponds to the sample, xy-plane being the sample's surface, the red coordinate system is attached to the crystallographic unit cell of the material.
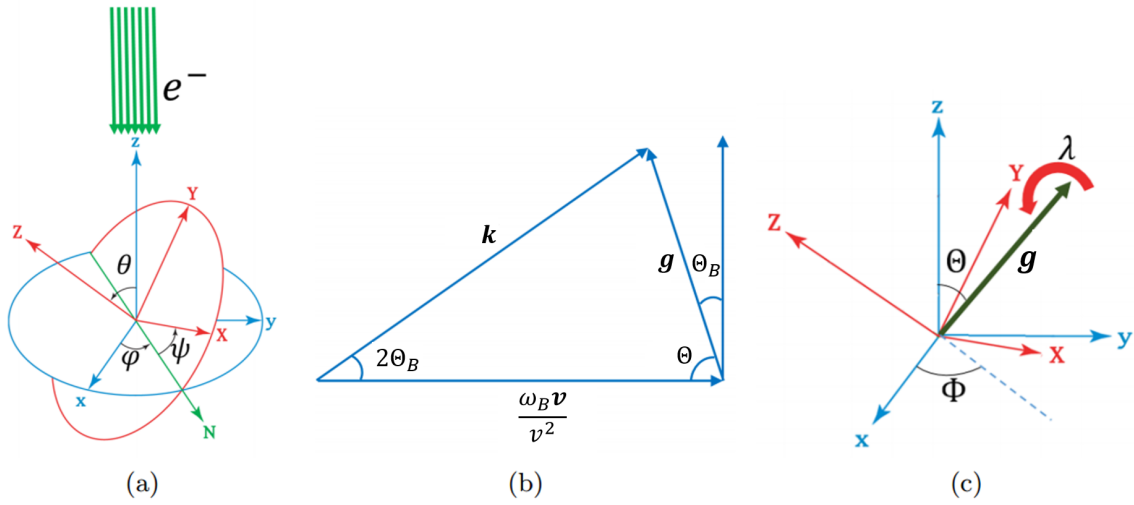

Figure 1. (a) Geometry of the problem, (b) Geometry of PXR, (c) The angles Φ, λ, Θ.

If the ODF is known, the distribution of PXR intensity resulting from interacting of relativistic electrons with polycrystal can be found. If one can use kinematical theory of PXR, which is justified for most cases of polycrystaline materials [15], the distribution of PXR intensity is given by (see [10] for more details):

$$I(\Theta, \Phi) = \frac{dN}{d\Phi d\Theta \sin\Theta} = T(|\boldsymbol{g}|, \Theta_B) \int_0^{2\pi} f(\varphi, \psi, \theta) d\lambda, \tag{2}$$

$$T(|\boldsymbol{g}|, \Theta_B) = \alpha L \frac{J}{e} \frac{|\cos 2\Theta_B|}{|\boldsymbol{g}|^3} |\kappa_g|^2 ((1 + \cos^2 2\Theta_B) \ln(\xi_{Deff} + \sqrt{\xi_{Deff}^2 + 1}) - \cos^2 2\Theta_B),$$

here N is a number of emitted photons, the introduced angles are shown in figure 1, φ, ψ, θ are expressed through Φ, λ, Θ, see [10] and figures 1a, 1c; $\xi_{Deff} = \gamma\theta_D$ and θ_D is the angular size of the detector (in radians); $\gamma = E/mc^2$ is the Lorentz factor of an electron with energy E; $\boldsymbol{g}$ is the reciprocal lattice vector, $\alpha = 1/137$, J is the electron beam current, e is the electron charge, L is the thickness of the polycrystal film, $\kappa_g = \chi_g(\omega)\omega^2/c^2$, κ_g does not depend on w with an appropriate accuracy, see [10]. $\omega, \chi_g(\omega)$ are the frequency and the X-ray susceptibility, respectively. Here for the convenience of further calculations we consider effective intensity I, which is a function of angles Θ, Φ. It is connected with observable intensity $I_0(2\Theta_B, \Phi)$ as

$$I = 4\sin\Theta_B I_0. \tag{3}$$

2

3. Inverse Problem

In this section we describe the way one can reconstruct ODF through measured angular intensity distribution. One can obtain experimentally measured $I_0(2\Theta_B, \Phi)$ from a group of reciprocal lattice vectors $\boldsymbol{g}$ with the same $|\boldsymbol{g}|$ by the method suggested in [10], employing a detector with narrow range of detectable energies. However, the last procedure should be elaborated as it was shown in [16–19] that at relatively low electron energies (conventionally $\gamma < 50$) the contributions of "side" reflexes [16] in the resulting intensity distribution are considerable. Thus, the intensity, related to the vectors $\boldsymbol{g}$ with the same $|\boldsymbol{g}|$, cannot be distinguished with appropriate accuracy. It is caused by widening of PXR peaks under low γ. Therefore we have to restrict the realm of application of the presented approach to electron energies, corresponding to $\gamma > 50$. Suppose one has experimentally measured $I_0(2\Theta_B, \Phi)$, then $I_1(\Theta, \Phi) = dN/d\Phi d\Theta \sin \Theta$ is calculated in a straightforward way by equation (3), $\Theta \in [0, \pi/2]$.

Below we make an assumption that ODF does not depend on ψ, that is $f(\varphi, \psi, \theta) \to f(\varphi, \theta)$. It corresponds to quite large class of fibre textures that are observed in thin film samples [20]. Let us rewrite equation (2) in detail taking into account the summation over $\boldsymbol{g}$ with the same $|\boldsymbol{g}| \equiv g$.

$$\frac{I(\Theta, \Phi)}{T(|\boldsymbol{g}|, \Theta_B)} = \sum_{\boldsymbol{g}:|\boldsymbol{g}|=g} \int_0^{2\pi} f(\varphi(\Theta, \Phi, \lambda, \boldsymbol{g}), \theta(\Theta, \Phi, \lambda, \boldsymbol{g})) d\lambda. \tag{4}$$

To proceed further let us use spherical function decomposition [20] and note a useful property of spherical function integration over the rotation around reciprocal lattice vector $\boldsymbol{g}$:

$$\int_0^{2\pi} Y_{lm}(\varphi(\Theta, \Phi, \lambda, \boldsymbol{g}), \theta(\Theta, \Phi, \lambda, \boldsymbol{g})) d\lambda = c_{lm}(z) Y_{lm}(\Theta, \Phi), \tag{5}$$

here $c_{lm}(z) = 2\pi i^m P_l(z)$ and $Y_{lm}(\theta, \varphi)$ is a spherical harmonic, $P_l(z)$ is a Legendre polynomial. $(x, y, z) = \boldsymbol{g}/|\boldsymbol{g}|$ in the red coordinate system. Thus, if we regard substitution $\varphi \to \varphi(\Theta, \Phi, \lambda, \boldsymbol{g}), \theta \to \theta(\Theta, \Phi, \lambda, \boldsymbol{g})$ and following integration over λ as an operator, say $\widehat{R}_g$ then Y_{lm} is its eigenfunction and c_{lm} is the corresponding eigenvalue. By virtue of equation (5) it follows from equation (4) that

$$(\frac{I}{T})_{lm} = \sum_{\boldsymbol{g}:|\boldsymbol{g}|=g} c_{lm}(z) f_{lm}. \tag{6}$$

Some of the coefficients in equation (6) vanish due to symmetry considerations, in particular if l is odd then $(\frac{I}{T})_{lm} = 0$. It happens because in this case $c_{lm}(z)$ is an odd function and in the summation in equation (6) for every $\boldsymbol{g}$ there is always $-\boldsymbol{g}$ as well. Therefore $\frac{I}{T}$ should be defined as

$$\frac{I}{T} = \begin{cases} \dfrac{I_1(\Theta, \Phi)}{T(\Theta)} & , \ \Theta \leq \dfrac{\pi}{2} \\ \dfrac{I_1(\pi - \Theta, \pi + \Phi)}{T(\pi - \Theta)} & , \ \Theta \geq \dfrac{\pi}{2} \end{cases}$$

Further simplifications can be obtained if one considers crystallographic symmetry of the material under study. As an example we will consider diamond-like crystal lattice, in this case it appears that $\sum_{\boldsymbol{g}:|\boldsymbol{g}|=g} c_{2m}(z) = 0$ for any $|\boldsymbol{g}|$. Hence we can determine only harmonics of $f(\varphi, \theta)$ with even (except for 2) l. Similar situation takes place for quantitative texture analysis based on x-ray diffraction pole figure measurement [20].

3.1. Nanodiamond film example

The ODF in equation (1) does not take into consideration lattice symmetries. In fact, there are orientations of the unit cell, say (φ, ψ, θ) and $(\varphi_1, \psi_1, \theta_1)$, that cannot be distinguished. Therefore, if one wants to find volume part of crystallites having orientation (φ, ψ, θ), then he has to add contributions corresponding to indistinguishable orientations as well. That is

$$\frac{dV}{V} = f(\varphi, \psi, \theta) \sin\theta d\varphi d\psi d\theta + f(\varphi_1, \psi_1, \theta_1) \sin\theta_1 d\varphi_1 d\psi_1 d\theta_1 +$$
$$... + f(\varphi_n, \psi_n, \theta_n) \sin\theta_n d\varphi_n d\psi_n d\theta_n \equiv F(\varphi, \psi, \theta) \sin\theta d\varphi d\psi d\theta, \tag{7}$$

Below we will seek for the function $F(\varphi, \psi, \theta)$, which under considered assumption turns into $F(\varphi, \theta)$ and use F as ODF. Consider two diamond lattice symmetries, that will let us find F from f_{lm}:

1) The rotation of the unit cell in figure 2a about X-axis by π and then about Z-axis by π results in equivalent orientation. Hence, one has to take the following combination instead of $f(\varphi, \theta)$

$$F_0(\varphi, \theta) = f(\varphi, \theta) + f(\varphi + \pi, \pi - \theta),$$

It appears that F_0 does not contain f_{lm} with odd l.

2) Another symmetry can be found if one considers elementary unit cell, see figure 2b. Green line represents the diagonal of cubic unit cell. There is one atom on it. The facets of the parallelepiped are identical rhombuses. Thereby, if one rotates it around its diagonal by $\pm 2\pi/3$ he gets initial unit cell and, consequently, lattice. Thus, there is a triad axis.
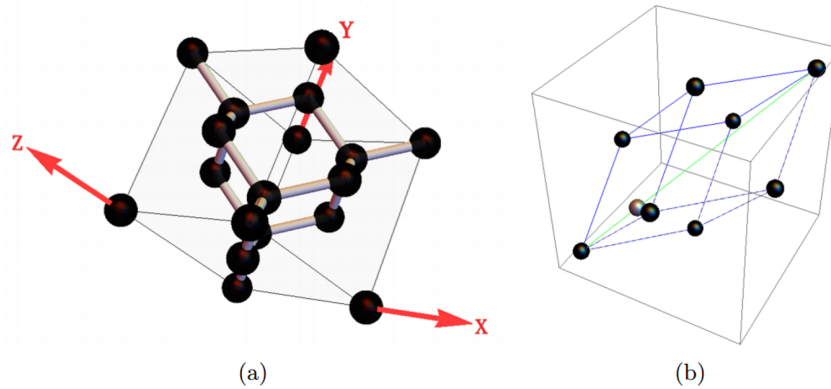

(a)   (b)

Figure 2. (a) Unit cell and attached frame of reference, (b) Elementary unit cell of the diamond lattice.

Mathematically, this triples the number of summands

$$F(\varphi, \theta) = F_0(\varphi, \theta) + F_0(\varphi^*, |\frac{\pi}{2} - \theta|) + F_0(\varphi + \frac{\pi}{2}, \frac{\pi}{2}),$$

where

$$\phi^* = \begin{cases} \varphi + \pi & , \theta \leq \frac{\pi}{2} \\ \varphi & , \theta \geq \frac{\pi}{2} \end{cases}$$

Eventually, it appears that F does not contain f_{2m}. That allows one to find F through even (except $l = 2$) harmonics of f that are known from equation (6). It is F that yields $dV(d\varphi, d\psi, d\theta)$ by virtue of equation (7). This formally allows to find ODF in terms of series in f_{lm}. It appears that for quite smooth ODFs several spherical harmonics (up to $l = 5$) are enough to get rather accurate solution.

The stability of the solution was tested. We modeled experimental intensity distributions by applying Poisson distribution to analytical solutions from Subsection 3.1 of [10]. We took the parameters of the polycrystalline diamond film from [21] and the electron beam from ASTA, Fermilab [22]. Then we found $F(\phi, \theta)$ by the above method. On the other hand, we had $F(\phi, \theta)$ expressed through initial $f_1(\varphi, \theta)$ (see [10]). See figure 3 for comparison of the results. In the plots z-axis corresponds to $F(\phi, \theta)$, in xy-plane we use polar coordinates. That is, the distance from the reference point $(x = 0, y = 0)$ equals $\theta(\text{rad})$, the angle ϕ is defined in a conventional way. It is seen in figure 3b that even if exposure time is as small as 1 second, one may obtain relatively good reconstruction of ODF. It results from considerable number of emitted photons $(\sim 10^6)$, which is an advantage. In figure 3c $F(\phi, \theta)$ is strongly distorted due to high deviations of number of emitted photons from its mean value at low exposure time (or number of incident electrons). Other parameters of the case: angular size of the detector $\theta_D = 0.033$ rad, maximal l (index in spherical harmonic) used in calculations of reconstruction $l_{\max} = 3$, parameters of initial ODF $\Theta_{pref} = 1.0$ rad, $S = 6.0$ (see [10]). It is crucial to note that F can be determined by
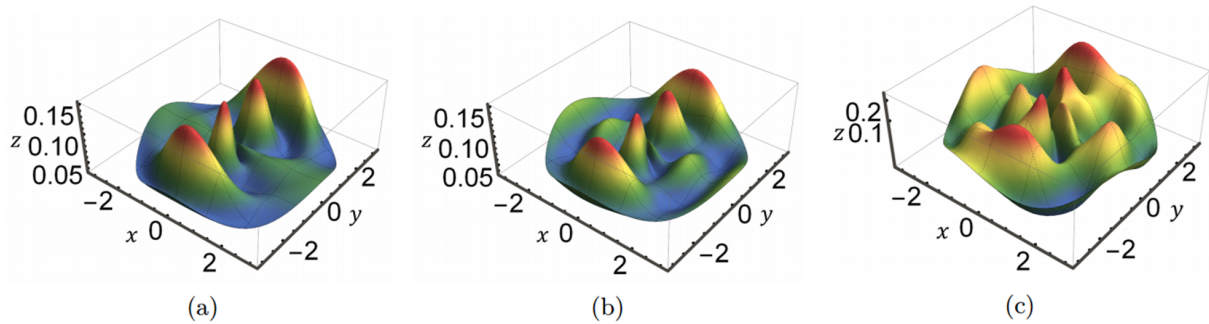

Figure 3. $z \equiv F(\phi, \theta)$, $x = \theta \cos \phi$, $y = \theta \sin \phi$. (a) Exact ODF, (b) Reconstructed, 6×10^{13} electrons (exposure time 1 sec), (c) Reconstructed, 6×10^8 electrons.

intensity distribution from all $\boldsymbol{g}$ that is easier to obtain on experiment (by direct measurement of angular intensity distribution without sorting out a contribution from a group of $\boldsymbol{g}$ with the same $|\boldsymbol{g}|$). Rewriting equation (2), but now summing over all $\boldsymbol{g}$ and taking into account structure of $T(|\boldsymbol{g}|, \Theta_B)$ one obtains

$$\frac{I(\Theta, \Phi)}{\alpha L \dfrac{J}{e} |\cos 2\Theta_B|((1 + \cos^2 2\Theta_B) \ln(\xi_{Deff} + \sqrt{\xi_{Deff}^2 + 1}) - \cos^2 2\Theta_B)} = $$
$$= \sum_{\boldsymbol{g}} \frac{|\kappa_g|^2}{|\boldsymbol{g}|^3} \int_0^{2\pi} f(\varphi(\Theta, \Phi, \lambda, \boldsymbol{g}), \theta(\Theta, \Phi, \lambda, \boldsymbol{g})) d\lambda. \tag{8}$$

Equation (8) is analogous to equation (4). Further derivation is essentially the same, though it is a little more cumbersome.

4. Discussion

To reconstruct the ODF based on the approach presented above one has to measure the angular distribution of x-ray yield. In contrast to x-ray diffraction pole figure measurement, no sample rotations are needed, and, provided with large area detector with moderate energy resolution, one can collect all the necessary information in one shot. Supposing ODF independent on ψ that would be enough for the ODF reconstruction. In case of electron beam with large spot size and realistically high current (like at [22]) the 1 sec exposure time is enough to obtain satisfactory statistics, so one potentially can apply this technique for in-situ investigations, e.g. texture changes due to temperature changes or stress.

Further investigation of the method will be the subject of subsequent publications. The generalization to the case of an arbitrary ODF will be the next step. Introducing another variable, such as the angle between the film's plane and the electrons' velocity (say β) might solve this problem.

5. Conclusions

Based on relation between ODF and the intensity distribution (equation (2)) the algorithm of determining ODF (independent on ψ) through the intensity distribution is described. It is based on expansion in series of spherical harmonics, several components (up to $l = 5$ for instance) being enough to preserve a good accuracy in case of rather smooth ODF. The solution proves to be stable (with respect to Poisson distribution of number of emitted quanta) at a large number of emitted photons ($\sim 10^6$ per sec) reachable at e.g. ASTA facility [22]. Described method does not need sample tilting as it requires only angular intensity distribution (if ODF does not depend on ψ), hence, in-situ texture changes may be potentially observed. Introducing another variable (measurement of intensity distribution at different angles β) may allow one to generalize the method to arbitrary ODF.

Appendix

Below we will provide some useful relations:

We'll make use of the rotation matrix

$$\begin{pmatrix} \cos\varphi\cos\psi - \cos\theta\sin\varphi\sin\psi & -\cos\theta\cos\psi\sin\varphi - \cos\varphi\sin\psi & \sin\theta\sin\varphi \\ \cos\psi\sin\varphi + \cos\theta\cos\varphi\sin\psi & \cos\theta\cos\varphi\cos\psi - \sin\varphi\sin\psi & -\sin\theta\cos\varphi \\ \sin\theta\sin\psi & \cos\psi\sin\theta & \cos\theta \end{pmatrix} \begin{pmatrix} X \\ Y \\ Z \end{pmatrix} = \begin{pmatrix} x \\ y \\ z \end{pmatrix} =$$

$$= \begin{pmatrix} \sin\Theta\cos\Phi \\ \sin\Theta\sin\Phi \\ \cos\Theta \end{pmatrix}, \tag{A.1}$$

(X, Y, Z) and (x, y, z) correspond to red and blue coordinate systems respectively.

Further,

$$Y_{lm}(\theta, \varphi) \sim \exp(im\varphi)P_l^m(\cos\theta) = \exp(im\varphi)\sin^m\theta\frac{d^m P_l(\cos\theta)}{(d\cos\theta)^m},$$

where P_l^m is an associated Legendre polynomial. Let us define

$$M_{lm}(t) = \frac{d^m P_l(t)}{dt^m}.$$

Add up first two lines in equation (A.1), the second being multiplied by i. This way, one immediately gets $\exp(i\Phi)$ on the right-hand side. Using connections between φ, ψ, θ and Φ, λ, Θ (see Appendix of [10]) one can find $\exp(i\varphi)$ on the other side as well

$$\exp(i\varphi)\sin\theta = \exp(i\Phi)(\sqrt{1-z^2}\sin\lambda + i(z\sin\Theta - \sqrt{1-z^2}\cos\Theta\cos\lambda)).$$

Again, from geometrical connections between angles one has

$$\cos\theta = z\cos\Theta + \sqrt{1-z^2}\sin\Theta\cos\lambda.$$

Thus, we have parts of $Y_{lm}(\theta,\phi)$ in a convenient form. An analogue of equation (5) takes the form

$$\int_0^{2\pi}(\sqrt{1-z^2}\sin\lambda + i(z\sin\Theta - \sqrt{1-z^2}\cos\Theta\cos\lambda))^m M_{lm}(z\cos\Theta + \sqrt{1-z^2}\sin\Theta\cos\lambda)d\lambda =$$
$$= c_{lm}(z)P_l^m(\cos\Theta).$$

We considered $m \geq 0$. The case $m \leq 0$ is essentially the same.

References

[1] Bunge H J 1982 *Texture Analysis in Materials Science* ed Bunge H J (Butterworth-Heinemann) p 294
[2] Wenk H and Van Houtte P 2004 *Reports on Progress in Phys.* **67** 1367
[3] Nikolayev D, Savyolova T and Feldmann K 1992 *Textures and Microstruct.* **19** 9
[4] Helming K 1998 *Materials science forum* vol 273 (Trans Tech Publ) p 125
[5] Matthies S, Wenk H R and Vinel G 1988 *J. Appl. Cryst.* **21** 285
[6] Chateigner D 2013 *Combined analysis* (John Wiley & Sons)
[7] Wenk H R 2006 *Rev. in Mineral. and Geochem.* **63** 399
[8] Mason J and Schuh C 2009 *Electron Backscatter Diffraction in Material Science* (Springer US) p 35
[9] Baryshevsky V G, Feranchuk I D and Ulyanenkov A P 2005 *Parametric X-ray Radiation in Crystals. Theory, Experiment and Applications* (Springer-Verlag)
[10] Lobach I, Benediktovitch A, Feranchuk I *et al.* 2015 *Nucl. Instrum. Meth.* B **360** 75
[11] Nasonov N N 1998 *Nucl. Instrum. Meth.* B **145** 19
[12] Blazhevich S, Chepurnov A, Grishin *et al.* 1999 *Phys. Lett.* A **254** 230
[13] Chouffani K, Andreyashkin M, Endo I *et al.* 2001 *Nucl. Instrum. Meth.* B **173** 241
[14] Nawang S, Endo I, Iinuma M *et al.* 2006 *J. Phys. Society of Japan* **75**
[15] Takabayashi Y, Endo I, Ueda K *et al.* 2006 *Nucl. Instrum. Meth.* B **243** 453
[16] Gogolev A S and Potylitsyn A P 2008 *Technical Phys.* **53** 1451
[17] Shchagin A, Pristupa V and Khizhnyak N 1990 *Phys. Lett.* A **148** 485
[18] Shchagin A and Khizhnyak N 1996 *Nucl. Instrum. Meth.* B **119** 115
[19] Feranchuk I D, Ulyanenkov A, Harada J *et al.* 2000 *Phys. Rev.* E **62** 4225
[20] Bunge H J 2013 *Texture analysis in materials science: mathematical methods* (Elsevier)
[21] Lobko A, Golubeva E, Kuzhir P *et al.* 2015 *Nucl. Instrum. Meth.* B **355** 261
[22] Sen T and Seiss T 2015 *arXiv preprint arXiv:1506.06719*